Combustion synthesis of zinc ferrite powders in oxygen

Yao Li [a,*], Jiupeng Zhao [b], Liangsheng Qiang [b], Jiuxing Jiang [a]

[a] *Center for Composite Materials, Harbin Institute of Technology, Harbin 150001, PR China*
[b] *Department of Applied Chemistry, Harbin Institute of Technology, Harbin 150001, PR China*

Abstract

The synthesis of zinc ferrite powders is carried out by combustion of a mixture of iron, iron oxides and zinc oxide powders in oxygen. An increase of oxygen pressure increases both the combustion temperature and velocity. The combustion reaction can not be self-sustained when the oxygen pressure is below 0.3 MPa. The results of XRD and Mössbauer spectroscopy show that intermediate phases of iron oxide, $Fe_{1-x}O$, $Fe_{1-z}O$ and crystal defects appear when the oxygen pressure is excessively low or high. An analysis of the dependence of the degree of conversion to ferrite on the oxygen pressure has been made. In addition, the reaction mechanism associated with the combustion synthesis (CS) of $ZnFe_2O_4$ is proposed.
© 2003 Elsevier B.V. All rights reserved.

Keywords: $ZnFe_2O_4$; Combustion synthesis; Oxygen pressure; X-ray diffraction

1. Introduction

Zinc ferrite belongs to the class of normal spinels. It is a commercially important material which is widely used in many industrial applications such as catalysis, photocatalysis, adsorption and pigment technologies [1,2]. The conventional methods for the preparation of $ZnFe_2O_4$ powders involve a solid state reaction of finely ground powders, heated at temperatures above at least $1100\,^\circ C$ for up to several hours and wet chemical methods such as sol–gel and hydrothermal methods [3,4]. These methods have multiple step pathways that are time consuming and expensive.

Recently, combustion synthesis (CS) or self-propagating high temperature synthesis (SHS) has been successfully used to speed up the synthesis of complex oxide materials, such as ferrite and high temperature superconductors [5,6], utilizing the potential advantages of low process cost, energy efficiency and short reaction time. In the literature, different ferrite systems synthesized by CS method have been reported: $Ni_xZn_{1-x}Fe_2O_4$ [5], $BaFe_{12}O_{19}$ [7] and $Li_{0.5}Fe_{2.5}O_4$ [8]. However, no systematic studies about phase transformation in the combustion wave and the reaction mechanism have been reported previously.

The main purpose of this work is to provide experimental information on the combustion synthesis of $ZnFe_2O_4$ from a powder mixture of ZnO, Fe and Fe_2O_3 in oxygen atmosphere. This work also involves the influence of the oxygen pressure on the degree of conversion to ferrite and the reaction mechanism of combustion synthesis of $ZnFe_2O_4$.

2. Experimental procedure

The raw materials used in preparation of $ZnFe_2O_4$ were iron, iron oxide, and zinc oxide, with an average particle size of 25, 0.8 and 0.5 μm, respectively. The purity of the raw materials is better than 99%.

The starting materials were weighed according to the required stoichiometric proportion, and were mixed in ethanol followed by ball milling for 8 h and then were dried in air. The mixture of powders were packed in a quartz container. A tungsten wire was used to initiate the reactants and the experiments were carried out in a water-cooled tube. Within a few seconds the combustion reaction was completed with the resultant white, loose products filling in the container which was then milled and $ZnFe_2O_4$ powders were obtained. The structure of CS chamber has been reported in a previous paper [9].

* Corresponding author. Tel.: +86-451-86412513;
fax: +86-451-86412513.
E-mail address: liyao@hit.edu.cn (Y. Li).

Combustion temperature and combustion wave velocity were measured with Pt/Rh thermocouples pressed into the mixture and registered. Phase transformation of the as-synthesized products were inspected by X-ray diffraction (XRD) (Siemens 5000). Morphology of the samples were characterized by scanning electron microscopy (SEM) (JSM 5410). The Mössbauer spectra of the $ZnFe_2O_4$ were recorded at room temperature using a constant acceleration Mössbauer spectrometer (Oxford MS-500, UK).

3. Results and discussion

3.1. Sample preparation

Synthesis of $ZnFe_2O_4$ ferrite proceeds according to the following reaction:

$$ZnO + (1-k)Fe_2O_3 + 2kFe + 1.5kO_2 = ZnFe_2O_4 \qquad (1)$$
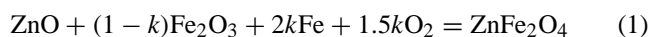
where k is the coefficient which controls the exothermicity of the mixture. The larger the k value, the higher is the molar ratio of $Fe:Fe_2O_3$ in the reactants. The combustion temperature (T_c) and combustion wave velocity (U_c) increase with the increase of the k value. Such results are in agreement with the earlier work [5].

The gaseous reactant, oxygen, also determines the processing parameters T_c and U_c. Fig. 1 shows the values of T_c and U_c under different oxygen pressures. With the increase of the oxygen pressure, T_c and U_c increase obviously. Moreover, the combustion temperature increases more strongly in the low oxygen pressure region than that in the high oxygen pressure region. The possible reason is that the oxygen permeability and proximity between particles are improved strongly with increasing the oxygen pressure in the low pressure region, accelerating the oxidation reaction of iron and increasing the quantity of the heat dispersed. Consequently, the combustion temperature increases strongly, increasing the driving energy for propagating the combustion wave.

The relationship between combustion temperature and reaction time under different oxygen pressures is shown in
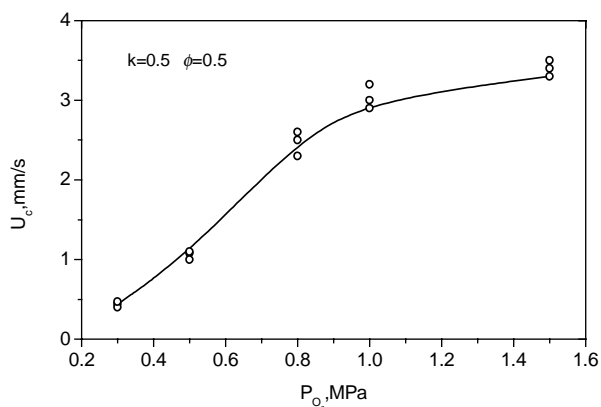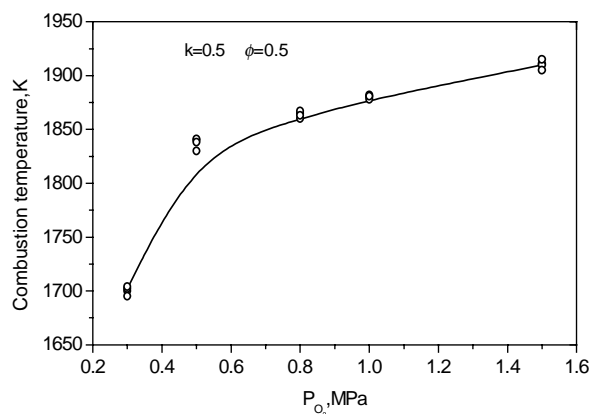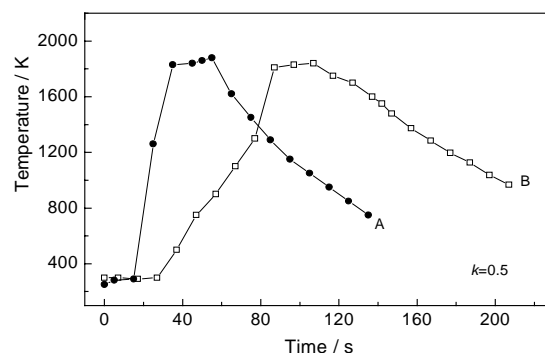
Fig. 2. The dependence of the combustion temperature on reaction time under different oxygen pressures. (A) $P_{O_2} = 1.0\,MPa$, (B) $P_{O_2} = 0.5\,MPa$.

Fig. 2. It should be noted that the temperature rises from the initial low temperature, up to 1840 K (a little above the melting point of Fe) and then at a much lower rate up to the maximum temperature of 1880 K (a little above the melting point of Fe_2O_3) for curve A. A similar phenomenon can be observed in curve B. Also, it can be seen from the temperature–time profile that the heating rate and the cooling rate at 1.0 MPa are much higher than those at 0.5 MPa due to the higher oxygen pressure.

Fig. 3 shows the propagation depth of the combustion front (the ratio of penetration depth of the combustion front, l, to the length of the reactant, L) versus the oxygen pressure. Under low oxygen pressures, the propagation depth of the combustion front increases asymptotically with the oxygen pressure. It has been found experimentally that the combustion of the samples ceases, not reaching the other end when the oxygen pressure is below 0.3 MPa. At low pressure of the gas, the available oxygen is not enough to sustain the oxidation of the ion and the pressure difference between the ambient medium and the powder pores is small which leads to the low penetration velocity of the oxygen into the inner, and the combustion ceases before it reaches the end. The relative error associated with the results shown in Figs. 1 and 3 is estimated to be 0.1 and 0.5%, respectively.
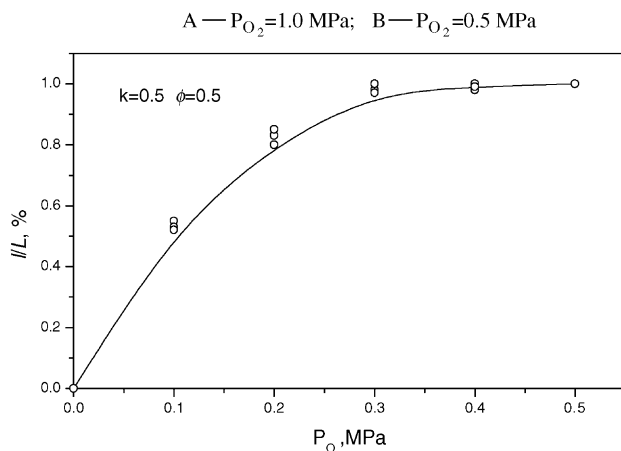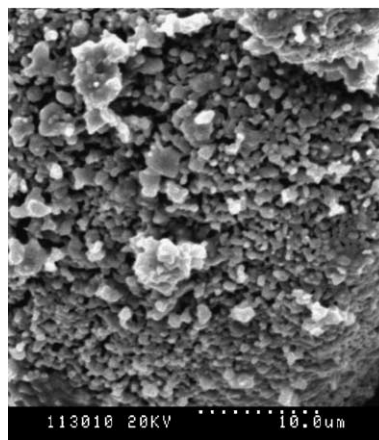
Fig. 1. Combustion temperature, combustion wave velocity versus oxygen pressure.

Fig. 3. Dependence of the propagation depth of the combustion front on the oxygen pressure.

Fig. 5. XRD patterns of the products synthesized under different oxygen pressures ($k = 0.5$, $\phi = 0.5$). (1) $P_{O_2} = 0.3$ MPa, (2) $P_{O_2} = 0.5$ MPa, (3) $P_{O_2} = 0.8$ MPa, (4) $P_{O_2} = 1.0$ MPa, (5) $P_{O_2} = 1.5$ MPa.
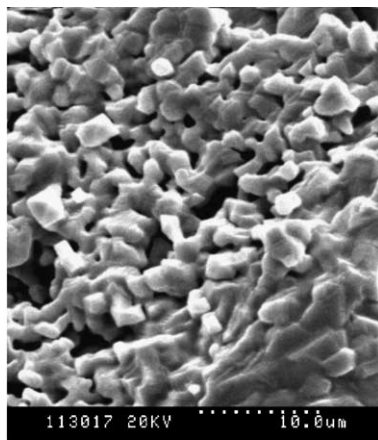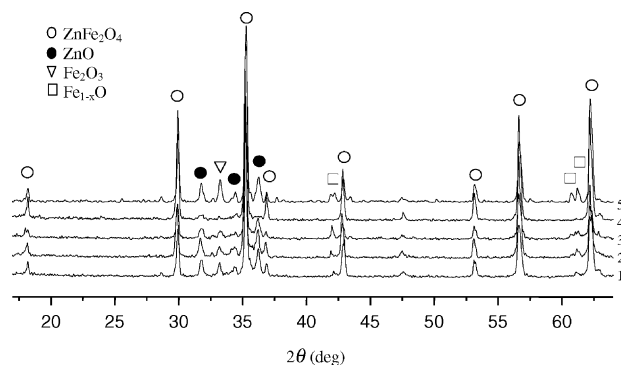
The final products are very loose and could be easily milled into powders. The crystalline degree of the combustion products obtained under 1.0 MPa is more perfect than that formed under 1.5 MPa as shown in Fig. 4. It clearly shows spherical-shaped particles for low oxygen pressure (1.0 MPa) and with a tendency towards an anomalous shape for higher oxygen pressure (1.5 MPa). The particle size increases substantially with the oxygen pressure due to the faster kinetics of the crystal growth under higher oxygen pressure. When oxygen pressure is above 1.5 MPa, the phase that has melted can be observed in the samples and the combustion product is very hard to be crushed into powders due to self-sintering.

3.2. X-ray powder diffraction and Mössbauer

Fig. 5 shows the XRD patterns of the combustion products under different oxygen pressures. At 0.3 MPa, besides the main lines of the ferrite matrix, additional lines belonging to the ZnO and α-Fe$_2$O$_3$ phases are seen in the XRD patterns.

Their intensity is highly dependent on the oxygen pressure. As the oxygen pressure increases from 0.3 to 1.5 MPa, the line intensity of α-Fe$_2$O$_3$ and ZnO decreases considerably. At 1.0 MPa, the diffraction peaks of ZnO and Fe$_2$O$_3$ disappear, and spinel peaks of ferrites can be clearly observed in the X-ray spectra of the products.

In addition, two diffraction lines, which exist at $2\theta = 42.2$ and $61.1°$, respectively, are attributable to a non-stoichiometric composition, Fe$_{1-x}$O ($x < 1$), deduced from the JCPDS card. However, the diffraction lines disappear when the oxygen pressure is increased to 1.0 MPa. When the oxygen pressure is 1.5 MPa, the corresponding diffraction lines split apart into a doublet which belongs to another non-stoichiometric phase, Fe$_{1-z}$O ($z < 1$).

The crystallite sizes calculated from X-ray line broadening using Scherrer's equation are in the range of 0.5–0.8 μm at 1.0 MPa and in the range of 2–3 μm at 1.5 MPa, indicating the growth of crystallite size with the increasing oxygen pressure.

Mössbauer spectra of the samples measured at room temperature are shown in Fig. 6. In Fig. 6(a), the doublet is related to ZnFe$_2$O$_4$ and the sextet is related to α-Fe$_2$O$_3$.

(a) $P_{O_2} = 1.0$ MPa

(b) $P_{O_2} = 1.5$ MPa

Fig. 4. SEM photomicrographs of the samples obtained under different oxygen pressures. (a) $P_{O_2} = 1.0$ MPa, (b) $P_{O_2} = 1.5$ MPa.
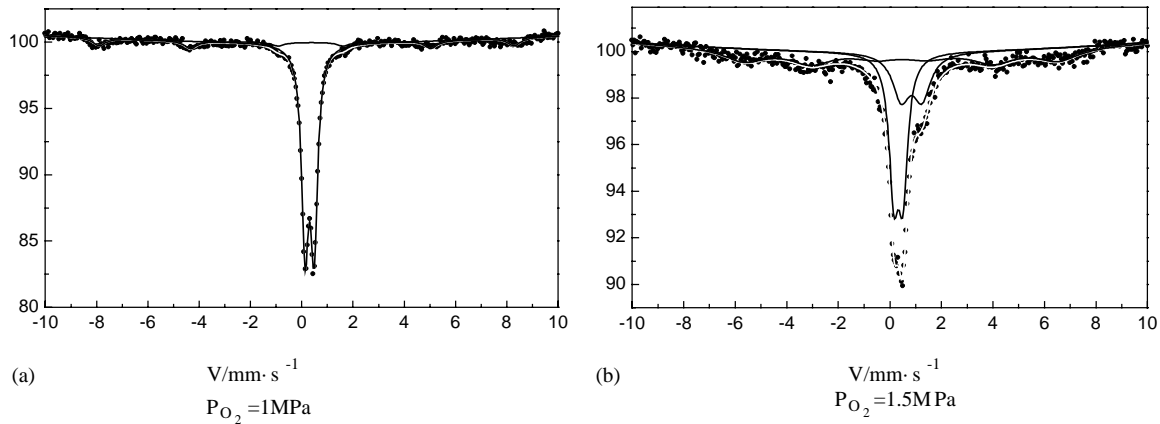
Fig. 6. Mössbauer spectra of the samples synthesized under different oxygen pressures. (a) $P_{O_2} = 1$ MPa and (b) $P_{O_2} = 1.5$ MPa.

In Fig. 6(b), the spectrum is built from three components: a sextet and two doublets. One of the doublets is also related to $ZnFe_2O_4$, the other is $Fe_{1-x}O$ or $Fe_{1-z}O$. While the sextet is close to γ-Fe_2O_3 according to reference [10]. The presence of γ-Fe_2O_3 indicates that the combustion products are formed under a high cooling rate due to the high combustion temperature under high oxygen pressure during the combustion reaction.

From the results of XRD and Mössbauer spectra analysis, it can be concluded that the non-stoichiometric composition, $Fe_{1-x}O$ or $Fe_{1-z}O$ is formed only under a very low or high oxygen pressure. A reasonable interpretation might be given as follows. When the combustion process is carried out under low oxygen pressure (below 1 MPa), the ferritization degree of the combustion products will be low due to the low T_c and U_c. When the oxygen pressure is high (above 1.5 MPa), the crystal lattice is distorted due to the high temperature and high combustion wave velocity. Therefore both a low and a high oxygen pressure would lead to a non-equilibrium condition under which some intermediate phases of iron oxide with a non-stoichiometric composition and crystal defects were formed. Similar results were obtained by Murin et al. during the oxidation of iron [11].

3.3. The effect of oxygen pressure on the degree of conversion to ferrite

If the combustion reaction is carried out under the low oxygen pressure, the ferritization degree of the combustion products will be low. This is caused by the shortage of oxygen and the lack of permeability. The degree of conversion to ferrite for the powders depends on the oxygen pressure and the porosity of the sample. Ideally, the amount of oxygen gas occupying the total volume of pores is stoichiometrically equal to that for the total conversion and is independent of the permeation of gas. We use the Clapeyron–Mendeleev equation to calculate their relationship, i.e.

$$P_{O_2}(\phi V) = n_{O_2} RT \tag{2}$$

where P_{O_2} is the oxygen pressure, ϕ the initial porosity of the sample, V the volume of the reactant, n_{O_2} the number of moles of O_2, ρ the density of iron, R the gas constant and T the combustion temperature.

According to Eq. (1), the molar volume of iron in the reactant, V_{Fe}, can be given as follows:

$$V_{Fe} = \frac{2k}{2+k} V \tag{3}$$

V_{Fe} also can be calculated as:

$$V_{Fe} = n_{Fe} \frac{M_{Fe}}{\rho} \tag{4}$$

where M_{Fe} is the atomic weight of iron, n_{Fe} the number of moles of iron in the reactants.

Suppose the combustion reaction is determined by the quantity of oxygen that penetrates into the pores, we define the parameter η as the degree of conversion to ferrite, and

$$\eta = \frac{n_{O_2}}{s n_{Fe}} \tag{5}$$

where s is the molar ratio of the oxygen to the iron during the complete oxidation of iron, and here $s = 3/4$. Combining Eqs. (2)–(5), η can be given as follows:

$$\eta = \frac{2(2+k)}{3k} \frac{M_{Fe}}{\rho R T_c} \frac{\phi}{1-\phi} P_{O_2} \tag{6}$$

Eq. (6) described the dependence of the degree of conversion on the oxygen pressure, porosity ϕ and combustion temperature. For a given porosity and combustion temperature, Eq. (6) simplifies to:

$$\eta = k_1 P_{O_2} \tag{7}$$

where k_1 is a constant, and

$$k_1 = \frac{2(2+k)}{3k} \frac{M_{Fe}}{\rho R T_c} \frac{\phi}{1-\phi} \tag{8}$$

It can be seen that the degree of conversion increases with the increasing oxygen pressure. Oxygen pressure corresponding to varying degrees of conversion to zinc ferrite
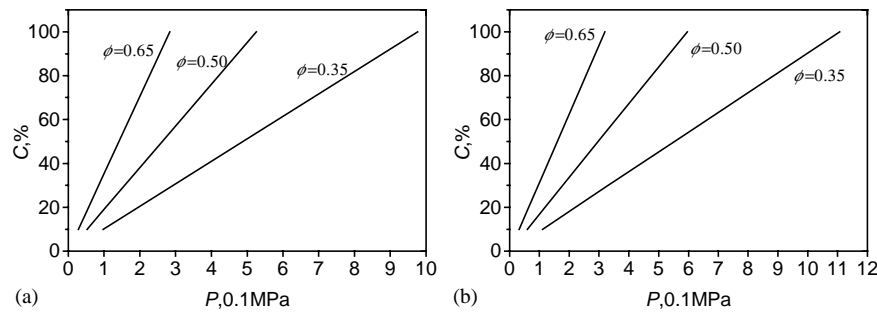
Fig. 7. Dependence of the degree of conversion to ferrite on oxygen pressure ($k = 0.5$). (a) $T_c = 1600$ K and (b) $T_c = 1800$ K.

were calculated by means of Eq. (6) for three porosity values and two temperatures. The results are shown in Fig. 7. The porosity range was selected to reflect practical upper and lower limits. The upper limit ($\phi = 0.65$) represents a value typical of uncompacted powders, while the lower limit ($\phi = 0.35$) is typical of highly compacted powders. Fig. 7(a) shows that in order to obtain complete conversion ($\eta = 1$), the oxygen pressure is raised from 0.28 MPa for $\phi = 0.65$ to 0.98 MPa for $\phi = 0.35$. For a given oxygen pressure, larger and more numerous pores of the reactant favours higher degree of conversion and lower dependence on the permeation of oxygen gas through the compact. For any given porosity and degree of conversion, higher pressure is required at higher temperature.

For a complete conversion and a given porosity, Eq. (6) becomes

$$P_{O_2} = \frac{3k}{2(2+k)} \frac{\rho R}{M_{Fe}} \frac{1-\phi}{\phi} T_c \tag{9}$$

Eq. (9) means that at a certain combustion temperature, there is a critical oxygen pressure value P_c. When the practical oxygen pressure is in excess of the critical value P_c, a complete conversion to ferrite can be obtained; while the practical oxygen pressure is lower than the critical pressure, the reactant will not be converted to ferrite completely due to the lack of oxygen.

3.4. Reaction mechanism

Steinberg et al. [12] proposed a mechanism for the burning of iron viz. that the iron was burned and the molten iron oxide was formed which was further oxidized to ferrite with higher molar oxygen-to-iron ratios than 1.5 for Fe_2O_3. Therefore, according to his result and the above analysis, the combustion reaction sequence of the Fe, ZnO and Fe_2O_3 system can be proposed as follows. During a combustion synthesis, the iron powder is ignited and is oxidized in a highly exothermic reaction which leads to a sharp increase in the temperature–time profile (Fig. 2). When the combustion temperature increases sharply, iron oxide in the reactants is formed from the burning iron and begins to melt, while the higher melting point particles such as zinc oxide, are suspended in the molten liquid. Intermediate phases, $Fe_{1-x}O$

and $Fe_{1-z}O$ appear due to the non-equilibrium phase transformation under the high heating rate. Then zinc oxide particles start to dissolve into the molten Fe_2O_3 through the interface and $ZnFe_2O_4$ grains precipitate out. As $ZnFe_2O_4$ is being formed, heat will continue to be produced by the oxidation of the unreacted iron powders. At this stage, the heat of oxidation causes the temperature of the reaction to continue to increase, although at a reduced rate, up to the maximum value (Fig. 2). As the oxidation of the iron powder continues, the quantity of unreacted iron decreases and ultimately disappears which means that the quantity of heat released decreases gradually. Accordingly, a sudden decrease in slope of the temperature–time profile appears which indicates that the sum of heat released by the oxidation of iron is less than that radiating to the environment.

When the temperature decreases to a certain value, zinc oxide will not dissolve any more into the melting liquid and react with Fe_2O_3 to form $ZnFe_2O_4$ because it lacks enough energy. As a consequence, ZnO remains in the combustion products as observed in EDX results (Fig. 8). The elemental analysis of the surface and inside of the products shows that the content of ZnO on the surface is higher than that of the inside, because of the lower temperature of the surface compared with the inside of the products.

From the analysis mentioned above, a model corresponding to the combustion reaction mechanism of $ZnFe_2O_4$ can be proposed as schematically shown in Fig. 9.
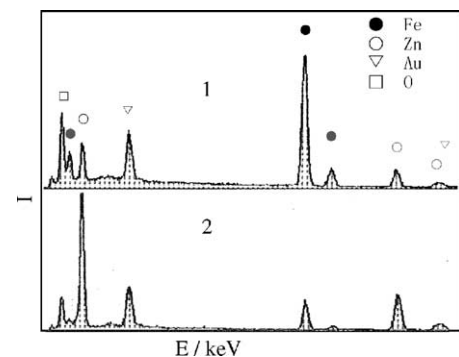

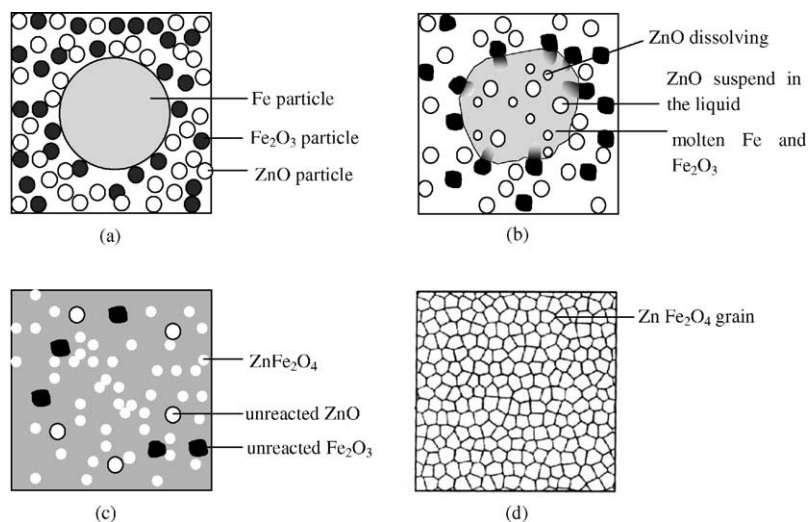Fig. 8. EDX patterns of the different part of the products. (1) Inside and (2) surface.

Fig. 9. A model of combustion synthesis of $ZnFe_2O_4$. (a) Reactants, (b) Fe and Fe_2O_3 particles melting, ZnO particles suspending and dissolving in the liquid, (c) $ZnFe_2O_4$ starting precipitation, and (d) combustion product.

4. Conclusions

The synthesis of zinc ferrite powders is carried out by combustion of a mixture of iron, iron oxides and zinc oxide powders in oxygen. Combustion temperature and combustion wave velocity increase with the increase of k value and oxygen pressure. Intermediate phases of iron oxide, $Fe_{1-x}O$, $Fe_{1-z}O$ and crystal defects appear when the oxygen pressure is excessively low or high. For a given porosity and combustion temperature, the degree of conversion to ferrite increases with increasing the oxygen pressure. A reaction mechanism of the combustion synthesis of zinc ferrite is also proposed according to the results of XRD, SEM and Mössbauer spectra.

References

[1] R.E. Ayala, D.W. Marsh, Ind. Eng. Chem. Res. 30 (1991) 55.
[2] J.F. Akyurtlu, A. Akyurtlu, Gas Sep. Purif. 9 (1995) 17.
[3] F.J. Guaita, H. Beltran, E. Cordoncillo, J.B. Carda, P. Escribano, J. Eur. Ceram. Soc. 19 (1999) 363.
[4] J.H. Lee, C.K. Kim, S. Katoh, R. Murakami, J. Alloys Comp. 325 (2001) 276.
[5] Y. Li, J.P. Zhao, J.C. Han, Mater. Res. Bull. 37 (2002) 583.
[6] A. Varma, J.P. Lebrat, Chem. Eng. Sci. 47 (1992) 2179.
[7] S. Castro, M. Gayoso, C. Rodriguez, J. Rivas, J. Mira, J.M. Greneche, J. Magn. Magn. Mater. 152 (1996) 61.
[8] F.B. Luis, V.K. Maxim, G.M. Yuri, A.P. Quentin, I.P. Parkin, Int. J. Inorg. Mater. 1 (1999) 311.
[9] Y. Li, J.P. Zhao, J.C. Han, Bull. Mater. Sci. 25 (4) (2002) 263.
[10] R.Z. Ma, Y.T. Xu, Mössbauer Spectroscopy, Science Press, Beijing, 1996, p. 328.
[11] I.V. Murin, V.M. Smirnov, G.P. Voronkov, V.G. Semenov, V.G. Povarov, B.M. Sinelnikov, Solid State Ionics 133 (2000) 203.
[12] T.A. Steinberg, J. Kurtz, D.B. Wilson, Combustion Flame 113 (1998) 27.